International Journal of Pharmaceutics 383 (2010) 161–169

Contents lists available at ScienceDirect

International Journal of Pharmaceutics

journal homepage: www.elsevier.com/locate/ijpharm

Note

Effects of extrusion process parameters on the dissolution behavior of indomethacin in Eudragit® E PO solid dispersions

Huiju Liu[a], Peng Wang[a], Xueyan Zhang[b], Fei Shen[c], Costas G. Gogos[a,*]

[a] Otto York Department of Chemical, Biological and Pharmaceutical Engineering, New Jersey Institute of Technology, Newark, NJ 07102, USA
[b] Material Characterization Laboratory, New Jersey Institute of Technology, Newark, NJ 07102, USA
[c] Polymer Processing Institute, Newark, NJ 07102, USA

ARTICLE INFO

Article history:
Received 8 June 2009
Received in revised form 28 August 2009
Accepted 2 September 2009
Available online 11 September 2009

Keywords:
Solid dispersion
Indomethacin
Eudragit® E PO
Batch mixer
Dissolution
Mixing

ABSTRACT

This work studied the dissolution of indomethacin (INM) into polymer excipient Eudragit® E PO (E PO) melt at temperatures lower than the melting point of INM using a laboratory-size, twin-screw counter-rotating batch internal mixer. The effects of three process parameters – set mixer temperature, screw rotating speed and residence time – were systematically studied. Scanning electron microscopy (SEM), optical microscopy (OM), X-ray diffraction (XRD) and Fourier transform infrared spectroscopy (FT-IR) were employed to investigate the evolution of INM's dissolution into the molten excipient. Differential scanning calorimetry (DSC) was used to quantitatively study the melting enthalpy evolution of the drug. The results showed that the dissolution rate increased with increasing the mixer set temperature, or the screw rotating speed. It was concluded that the dissolution of the drug in the polymer melt is a convective diffusion process, and that laminar distributive mixing can significantly enhance the dissolution rate. More importantly, the time needed for the drug to dissolve inside the molten polymer and the typical residence time for an extrusion process fall in the same range.

1. Introduction

There is a strong interest from both academia and the pharmaceutical industry to utilize hot melt extrusion (HME) to prepare drug–polymer solid dispersions or solid solutions, which have the potential to dramatically increase the dissolution rate and, thus, the bioavailability of the drugs with poor aqueous solubility (Hulsmann et al., 2000; Leuner and Dressman, 2000; Crowley et al., 2007). Compared to other processing methods, the HME has advantages such as the elimination of the solvent usage and involves fewer processing steps. On the other hand, because materials are heated during the HME, thermal degradation of the active pharmaceutical ingredients (APIs) has been a general concern (Breitenbach, 2002; Repka et al., 2007). Many APIs are heat sensitive, especially at temperatures above their melting point (Verreck et al., 2006).

Naturally, a strategy to circumvent the thermal degradation issue is to decrease the processing set temperature. For example, the solid dispersions or solid solutions can be made at temperatures lower than the drug's melting point (Chokshi et al., 2008; Qi et al., 2008). In those cases, the solid drug may gradually dissolve into the polymer excipient melt, resulting in a desirable polymer–drug system where the API is in an amorphous, albeit possibly metastable, state. Nakamichi et al. reported that kneading blocks play a key role in transforming the crystalline nifedipine to an amorphous form in hydroxypropylmethylcellulosephthalate (HPMCP) and pointed out the importance of the screw speed (Nakamichi et al., 2002). Shibata et al. studied the preparation of solid solution of indomethacin with crospovidone using a twin-screw extruder, and concluded that the residence time, screw speed and heating temperature are significant factors (Fujii et al., 2005; Shibata et al., 2009). Although the process has been studied in several previously published articles, more research is needed to understand the underlying dissolution mechanism from polymer mixing perspective and how to promote the dissolution process.

Extrusion technology has been used in polymer industry over 80 years, and a great wealth of knowledge has been accumulated on the polymer laminar mixing phenomena taking place in extruders, both in theory and practice during the past several decades. The mixing processes in single and twin-screw extruders are generally categorized into two types: dispersive mixing and distributive mixing (Tadmor and Gogos, 2006). During dispersive mixing, a critical stress has to be supplied by the laminar flow of the molten excipient generated by the extruder, to overcome the cohesive forces of liquid droplets or agglomerated particulates, so that the size of the dispersed phase can be reduced. In contrast, distributive mixing is more effectively carried out by flows that generate large strains,

* Corresponding author. Tel.: +1 973 596 8449; fax: +1 973 642 4594.
E-mail address: costas.g.gogos@njit.edu (C.G. Gogos).

0378-5173/$ – see front matter © 2009 Published by Elsevier B.V.
doi:10.1016/j.ijpharm.2009.09.003

such as extensional and stream-splitting flows, and there is no critical stress needed to be overcome. To facilitate distributive mixing, screw elements are often designed to split and reorient the streams for better mixing. In this drug–polymeric excipient mixing study, the drug is dissolvable in the polymer melt. Both dispersive mixing and distributive mixing may promote the dissolution process of drugs into polymeric melt. Thus, it is of great interest to find out how dispersive mixing and distributive mixing and different process parameters, such as the screw rotating speed, the mixer setting temperature and the residence time, affect the final products' properties.

In this study, a batch mixer is used to experimentally investigate the effects of extrusion process parameters on the drug–polymer mixing. The batch mixer is a heated high shear laminar mixer, which has been extensively used in the plastics and rubber industry to simulate the extrusion process or optimize the formulation. Batch mixers require only 30–60 g of the material and many experiments can be performed in a short period, thus making the batch mixer an attractive choice for the HME study (Ghebre-Sellassie and Martin, 2007). Furthermore, the screw speeds can be controlled separately without altering the residence time in a batch mixer, which is difficult to realize if an extruder is used.

INM and E PO were chosen as the model API and the model excipient polymer, respectively. INM is a non-steroidal anti-inflammatory drug with a $pK_a = 4.5$, commonly used to reduce fever, pain and swelling. It has a poor and pH-dependent water solubility (4.0–8.8 μg/mL in water) (Zhu et al., 2006). E PO is a copolymer composed of neutral methyl and butyl methacrylic acid esters, and dimethylaminoethyl methacrylate repeating units. This polymer is soluble up to pH 5 and above this pH value is capable of swelling and being permeable to water. The system of E PO and INM has been studied by solvent method (Filippis et al., 1991; Lin and Perng, 1993) and melt method (Chokshi et al., 2005).

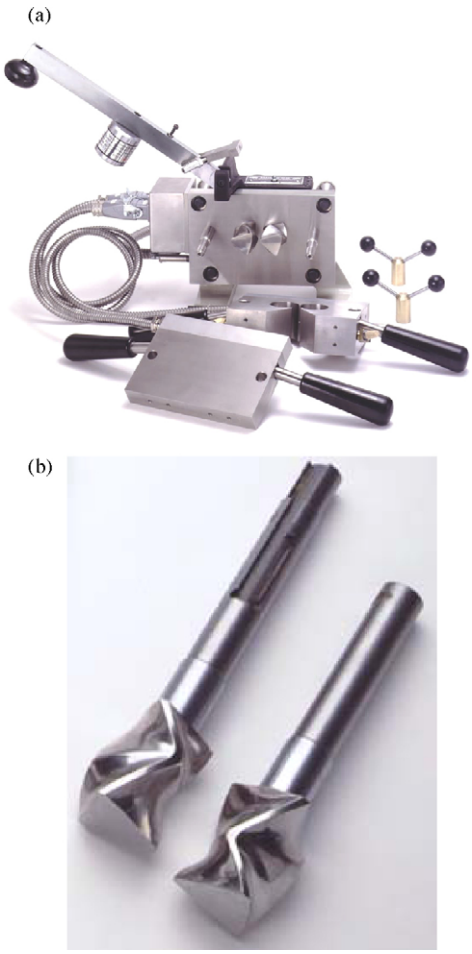

Fig. 1. A batch mixer and roller screws (reprinted with permission from Brabender).

2. Materials and methods

2.1. Materials

E PO ($M_w = 47{,}000$) was donated by Evonik Industries (Piscataway, NJ). INM was purchased from Spectrum Chemicals & Laboratory Products (Gardena, CA). The weight ratio of E PO to INM is kept constant at 70:30 in this study.

2.2. Sample preparation

A physical mixture was obtained by pre-mixing INM and E PO at room temperature for 25 min at 250 rpm, using a jar rolling mill (JRM 2″ × 24″, Paul O. Abbe Inc.). After mixing, three random samples were examined by differential scanning calorimetry (DSC) and thermal gravimetrical analysis (TGA). A high repeatability of the DSC and TGA measurement results was found among the random samples, indicating a good uniformity of the physical particle/particle mixtures.

All the runs were performed in a Brabender FE-2000 batch intensive mixer utilizing counter-rotating screws, as illustrated in Fig. 1. The batch mixer is heated electrically and cooled by air. The melt temperature sensor measures the actual melting material's temperature; the torque meter can record the resistance of material to the flow created by the rotation of the screws. Generally, about 70–75 vol.% fill degree of the chamber is recommended for good mixing. The free volume in the mixing chamber is 60 cm^3. The density of INM and E PO is 1.34 and 1.1 g/mL, respectively (Marsac et al., 2009). Thus, 50 g of the physical mixture was used for every run to achieve 70% fill degree. The mixture was introduced into the batch mixer by a feeding chute. The processing conditions are outlined in Table 1.

The screw speed of the batch mixer was set using a computer program; the machine automatically stopped for 10 s for sampling at the designed residence (mixing) times of 50, 95, 140, 280 and 420 s. About 0.3–0.5 g samples were taken out at each sampling time, and the samples were labeled 55, 100, 145, 285 and 420 s accordingly.

2.3. Differential scanning calorimetry (DSC)

DSC Q100 from TA Universal Instruments was used to conduct DSC tests. The samples were ground into fine powders by a pestle and mortar. About 4–8 mg powder sample was accurately weighed, placed in an aluminum pan and crimped with an aluminum lid. The heating rate was 20 °C/min from 0 to 180 °C under nitrogen flow (40 cm^3/min) for all samples. The DSC data were analyzed by using Universal Analysis 2000 software.

Table 1
Experimental conditions.

Run	Set temperature (°C)	Screw speed (rpm)	Sampling time (s)
1	100	20	55
2	100	100	100
3	110	20	145
4	110	100	285
5	140	20	420

2.4. X-ray diffraction (XRD)

XRD analysis was performed for raw materials, physical mixture and all the samples taken from the batch mixer with a Philips PW3040 X-ray diffractometer (Cu Kα radiation, 0.154 nm), operated at 45 kV/40 mA. The raw materials and physical mixtures were in powder form, whereas the samples taken from the batch mixer were compressed into films (thickness 0.05 mm) at 75 °C with a compression molding machine. The samples were analyzed in the 2θ range from 5 to 30° using a 0.03° step size with a 1-s dwell time at each step.

2.5. Optical microscopy

An optical microscope (Carl Zeiss Universal Research Microscope) was used to characterize the samples' morphology. The Zeiss Axiocam Digital camera has 5 MB pixel resolution. The samples taken from the bath mixer were compressed into films for microscopy observation (thickness 0.05 mm) at 75 °C with a compression molding machine.

2.6. FT-IR spectroscopy

FT-IR spectroscopy was performed using a Perkin Elmer Spectrum One FT-IR-Spectrometer and the KBr method in the 4000–400 cm^{-1} region at 4 cm^{-1} resolution and 25 scans per spectrum. The samples were ground with KBr powder into fine powders by a pestle and mortar; the weight percent of samples in the KBr pellet was 1.3–1.5%.

2.7. Dissolution test

Dissolution properties were performed at 37 °C using a Distek dissolution system 2100A with a Distek temperature control system TCS 0200 according to USP Dissolution Apparatus II with the paddle rotation speed of 50 rpm. The dissolution medium was 900 mL of pH 1.2 hydrochloric acid buffer solution. Samples obtained from the batch mixer were compressed into 2 mm thick sheets for the dissolution test. Dissolution samples equivalent to 28 mg of drug were added to the dissolution apparatus, and the test fluid was collected at predetermined time intervals, filtered through a 0.45 μm filter and then analyzed at 320 nm by an Agilent 8543 UV–vis spectroscopy system with a photodiode array detector. The experiments were conducted in triplicate.

3. Results and discussion

3.1. Mixing torque traces

Mixing torque traces and the melt temperatures from the Brabender batch intensive mixer for four runs are shown in Fig. 2. The torque traces give much information about feeding, melting, mixing and rheological properties. The torque fluctuation before the point of the maximum torque represents the feeding surge and/or the occurrence of melting on the polymer particle surface. The dramatic decrease of torque after the maximum torque suggests rapid and uniform melting of the polymer particles. The equilibrium torque is associated with the apparent viscosity of the drug–polymer melt mixture. The disparity between the set temperature and the actual melt temperature is related to flow induced viscous energy dissipation, which depends on the mixture viscosity and the screw speed.

For a given screw speed, the torque decreases as the set temperature increases because the melt viscosity drops with the rising of the melt temperature. The final torque for the condition at 100 °C 20 rpm is over two times higher than that at 110 °C 20 rpm, whereas

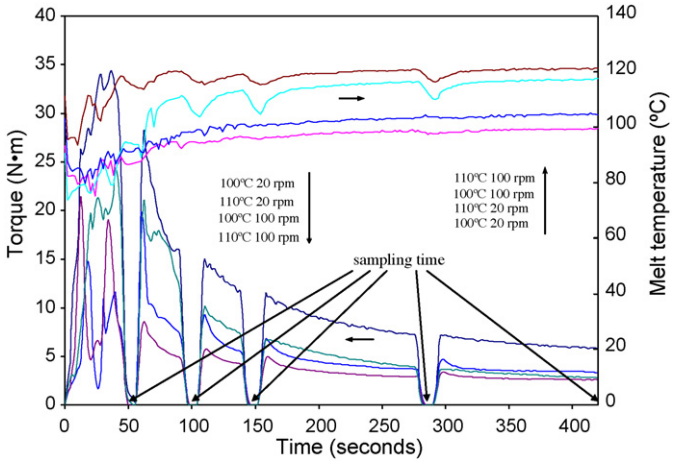

Fig. 2. Mixer torque traces and the measured melt temperature curves.

the final torque for the condition at 100 °C 100 rpm is only 30% higher than that at 110 °C 100 rpm. The larger difference of the final torques between 100 and 110 °C at 20 rpm results from the large difference of the melt viscosity between these two temperatures at low shear rate. Specifically, the shear thinning effect may not occur or begin to manifest at a very low shear rate corresponding to 20 rpm. In contrast, the temperature-induced difference becomes much smaller at 100 rpm because of the stronger shear thinning effect at the higher shear rate.

For the same mixer temperature, the torque decreases as the screw speed increases. There are two reasons for this observation: on the one hand, the higher screw speed corresponds to a higher shear rate, which leads to a more pronounced shear thinning effect, causing lower viscosity and lower torque; on the other hand, more viscous dissipation heat will be generated at higher screw speeds, increasing the melt temperature and lowering the torque. It is worth emphasizing that viscous dissipation heat may make a significant contribution to the torque decrease: the final melt temperature increases from 99.6 °C for the 100 °C 20 rpm condition to 117.4 °C at 100 °C 100 rpm; the final melt temperature increases from 104.7 °C for the 110 °C 20 rpm condition to 121.3 °C at 110 °C 100 rpm. In other words, the actual melt temperature increases almost 20 °C at either set temperature if the screw speed changes from 20 to 100 rpm.

3.2. DSC results

Two representative DSC curves of the samples processed at 100 °C 20 rpm and 140 °C 20 rpm are shown in Fig. 3. In each run, the specific enthalpy (enthalpy/total drug mass) needed for melting the remaining INM particles decreases as the residence time increases. There are still endothermic peaks on the DSC curves for the 420 s samples for the mixing conditions at 100 °C 20 rpm and 110 °C 20 rpm. The endothermic peaks disappear at 285, 285 and 145 s, for mixing at 100 °C 100 rpm, 110 °C 100 rpm and 140 °C 20 rpm, respectively.

The principal melting peak of the physical mixture corresponds to the γ-form INM (Slavin et al., 2002). The endothermic enthalpy of INM can be used to compare with that of INM in the physical mixture (59.7 J/g) to roughly determine the proportion of the undissolved drug, i.e., the crystalline drug. This calculation indicates that there are still 5.67 and 2.51% undissolved drug particulates in the mixture at the end of processing for the condition of 100 °C 20 rpm and 110 °C 20 rpm, respectively.

Interestingly, the endothermic peak of INM is significantly different in the pure drug and the physical mixture (PM) shown

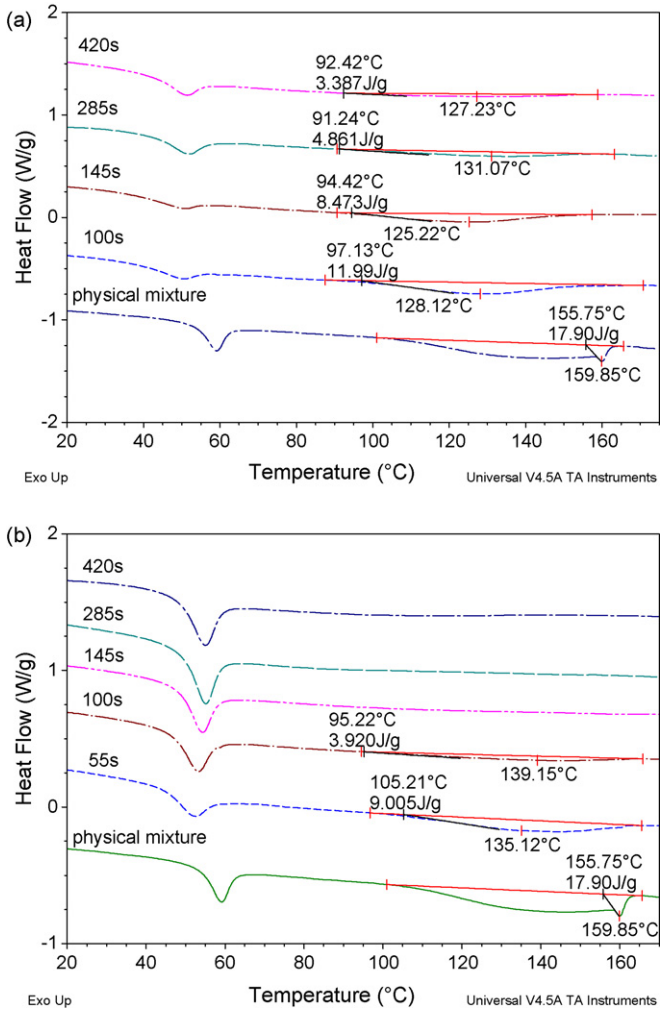

Fig. 3. DSC curves of the samples prepared at: (a) 100 °C 20 rpm and (b) 140 °C 20 rpm.

in Fig. 4. The melting peak of the pure drug is typically sharp, whereas the endothermic peak in the physical mixture becomes much broader. As compared to the specific enthalpy of the pure drug (108.4 J/g), the enthalpy of the drug in the physical mixture becomes 59.7 J/g at the scanning rate of 20 °C/min. The enthalpy increases somewhat from 59.7 to 61.2 J/g when the scanning rate increases from 20 to 60 °C/min. The phenomenon has been reported

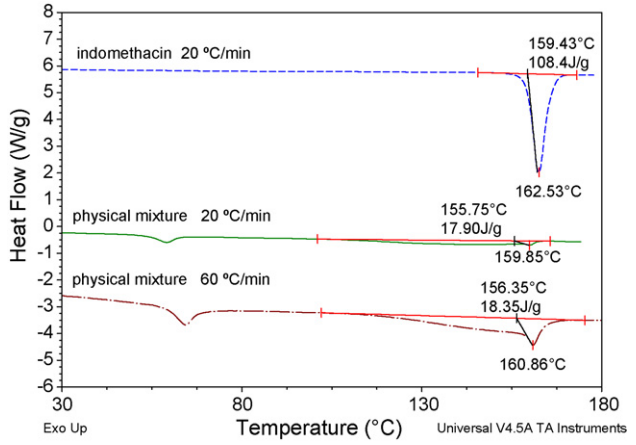

Fig. 4. DSC curves of the pure drug and the physical mixture sample.

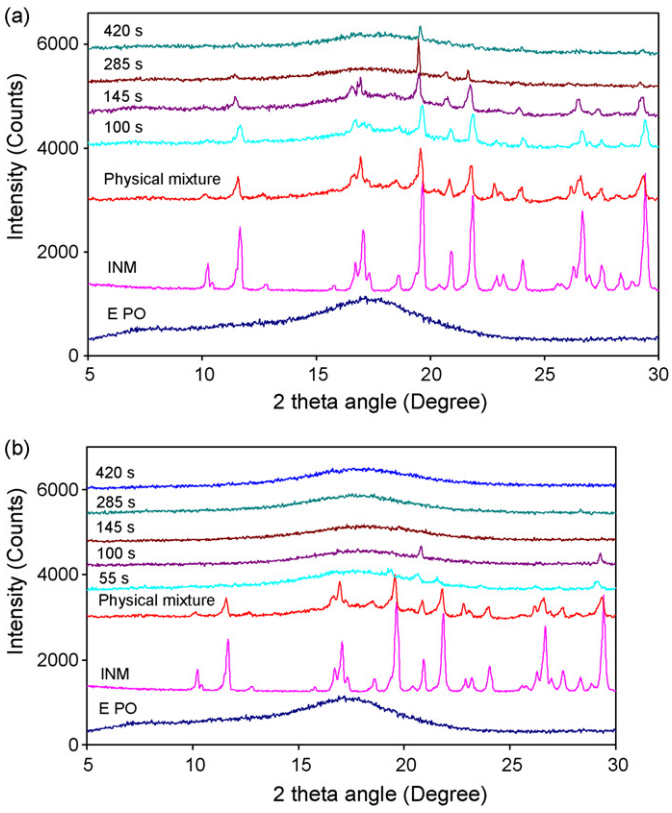

Fig. 5. XRD patterns of runs at: (a) 100 °C 20 rpm and (b) 140 °C 20 rpm.

for other systems by several groups recently (Qi et al., 2008; Tao et al., 2009). Craig et al. ascribed the broadness of endothermic peak to the gradual dissolution of the drug in the polymer during the DSC heating ramp, and ascribed the increased specific enthalpy at the higher scanning rate to reduced time for dissolution in the molten polymer and thus a remaining larger proportion of the drug in the solid state, which subsequently melts (Qi et al., 2008). The findings in this study are in agreement with this explanation.

3.3. XRD analysis

Fig. 5 shows the evolution of XRD patterns of the representative samples at the mixing conditions of 100 °C 20 rpm and 140 °C 20 rpm. The crystallinity peak of INM becomes weaker and weaker as the residence time increases in the same run. The crystallinity peak still exists at 420 s for samples processed at 100 °C 20 rpm and 110 °C 20 rpm. The peak disappears at 285, 145 and 145 s for runs at 100 °C 100 rpm, 110 °C 100 rpm and 140 °C 20 rpm, respectively.

3.4. Morphology observations

Figs. 6 and 7 show optical micrographs of samples processed at 100 °C 20 rpm and 110 °C 100 rpm. The amount of the drug particles decreases with the processing time. For the run at 100 °C 20 rpm, both optical micrographs and SEM pictures (not shown) show that there are still considerate amounts of drug particulates which were not dissolved for the 420 s sample, whereas for the run at 110 °C 100 rpm, both optical micrographs and SEM pictures (not shown) show that essentially no drug particulates can be found in the 285 s sample. The morphology observation is in agreement with DSC and XRD data.

The micrographs of samples processed at 110 °C 20 rpm (not shown) are similar to the graphs at 100 °C 20 rpm, and the micro-

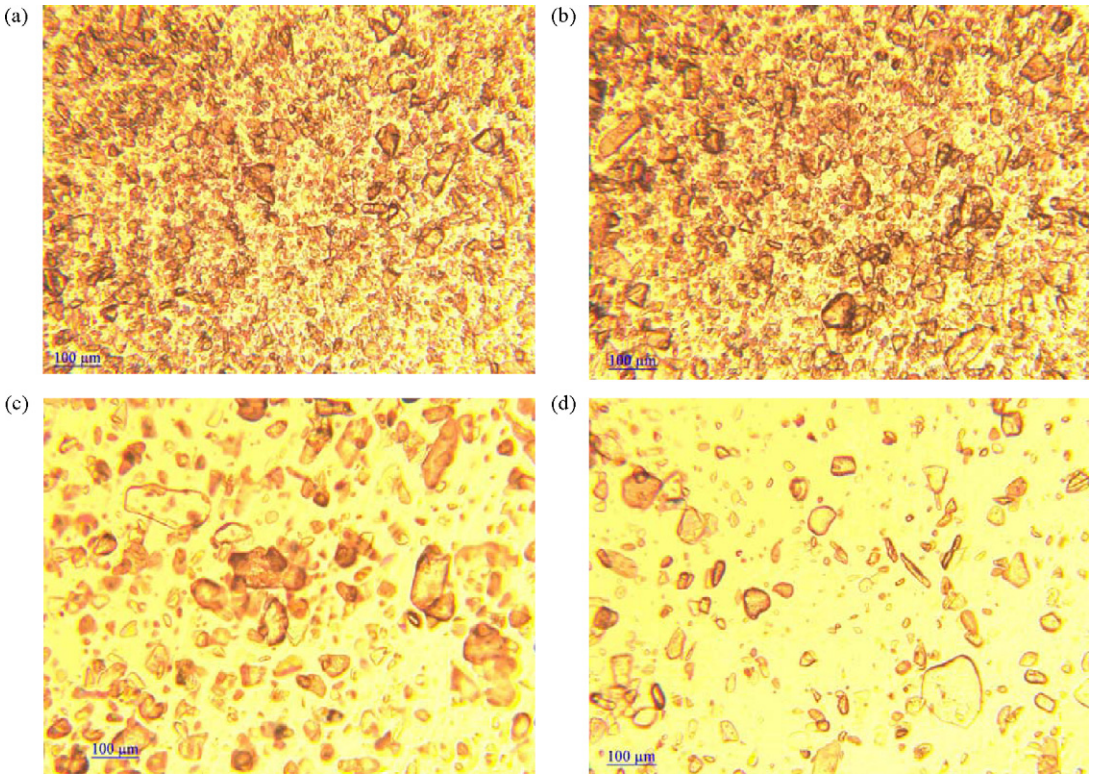

Fig. 6. Optical micrographs of run at 100 °C 20 rpm.

graphs of samples processed at 100 °C 100 rpm and 140 °C 20 rpm are similar to the graphs at 110 °C 100 rpm (not shown).

3.5. FT-IR analysis

FT-IR studies were conducted on every sample to further confirm the crystalline state of the drug in the mixture, as shown in Fig. 8. Taylor and Zografi have obtained two polymorphs of INM with their main IR absorption peaks at 1735, 1688, 1681 and 1649 cm^{-1} for the α-form, at 1717 and 1692 cm^{-1} for the γ-form, and at 1710 and 1684 cm^{-1} for the amorphous INM. The carboxylic acid groups hydrogen bond to form cyclic dimers in the γ-form and amorphous INM (Kistenmacher and Marsh, 1972), and the asymmetric carboxylic acid C=O stretch of cyclic dimers in them is corresponding to the peaks at 1717 and 1710 cm^{-1}, respectively. Furthermore, the peaks at 1692 and 1684 cm^{-1} are assigned to benzoyl C=O stretch for the γ-form and amorphous INM, respectively (Taylor and Zografi, 1997). Thus, the abovementioned peaks can be utilized to characterize the drug state in the mixture. In this study, the original crystalline drug particles are in γ-form.

For the samples processed at 100 °C 100 rpm shown in Fig. 8a, the peak at 1692 cm^{-1} shifts to 1683 cm^{-1}, and the sharper peak at 1692 cm^{-1} becomes broader at 1683 cm^{-1}, which indicates that the original γ-form was converted to amorphous INM. In addition, the peak at 1718 cm^{-1} shifts to high wavenumber and eventually to 1732 cm^{-1} corresponding to the non-hydrogen bonded C=O stretch for amorphous INM and E PO (Lin and Perng, 1993; Taylor and Zografi, 1997). The carboxylic acid dimers were mostly disrupted by the molecular interactions between INM and E PO because no peak appeared at 1710 cm^{-1}, which is assigned to the C=O stretch of cyclic dimmers for amorphous INM. The time needed for the transformation into the amorphous form is 285, 145 and 145 s for conditions of 100 °C 100 rpm, 110 °C 100 rpm and 140 °C 20 rpm, respectively.

For the samples processed at 110 °C 20 rpm shown in Fig. 8b, the peak at 1692 cm^{-1} shifts slightly to 1689 cm^{-1}. Although the sharper peak at 1692 cm^{-1} becomes broader at 1689 cm^{-1}, the mixture must still have some crystallized drug particulates because the final peak is still away from the characteristic peak of the amorphous INM. Moreover, the peak at 1718 cm^{-1} shifts to 1729 cm^{-1} rather than to 1732 cm^{-1}, which implies that the carboxylic acid dimers were partly disrupted by the molecular interactions between INM and E PO.

3.6. Dissolution test

Dissolution profiles of INM from the 420 s samples at different conditions are shown in Fig. 9. Every sample attains a maximum percentage release at approximately 20 min due to the fast dissolution of E PO at such low pH medium. Initially, the dissolution rates of five samples are very close, and increase by about 20-fold as compared to the pure drug and 10-fold as compared to the corresponding physical mixture. In spite of the recrystallization, the apparent equilibrium solubility of the drug measured from the HME samples was still 5.5-fold that of the pure drug.

Precipitation of the drug from the dissolution solution was noticed for every sample. The sample processed at 140 °C 20 rpm could stay in the supersaturated state for 100 min after above 90% release, whereas, for the other four samples, the drug gradually precipitated once the release percentage attained its peak. The drug precipitation was observed for the same system by several other research groups (Filippis et al., 1991; Chokshi et al., 2008). This phenomenon might be correlated to the state of the drug present in the mixture; in conjunction with other physicochemical data, the dissolution test can provide strong evidence for the formation of a "molecularly dispersed or nearly molecularly dispersed system" (Leuner and Dressman, 2000). In the supersaturated aqueous solution, the drug molecules may easily nucleate and precipitate, if there are some small crystalline particulates or

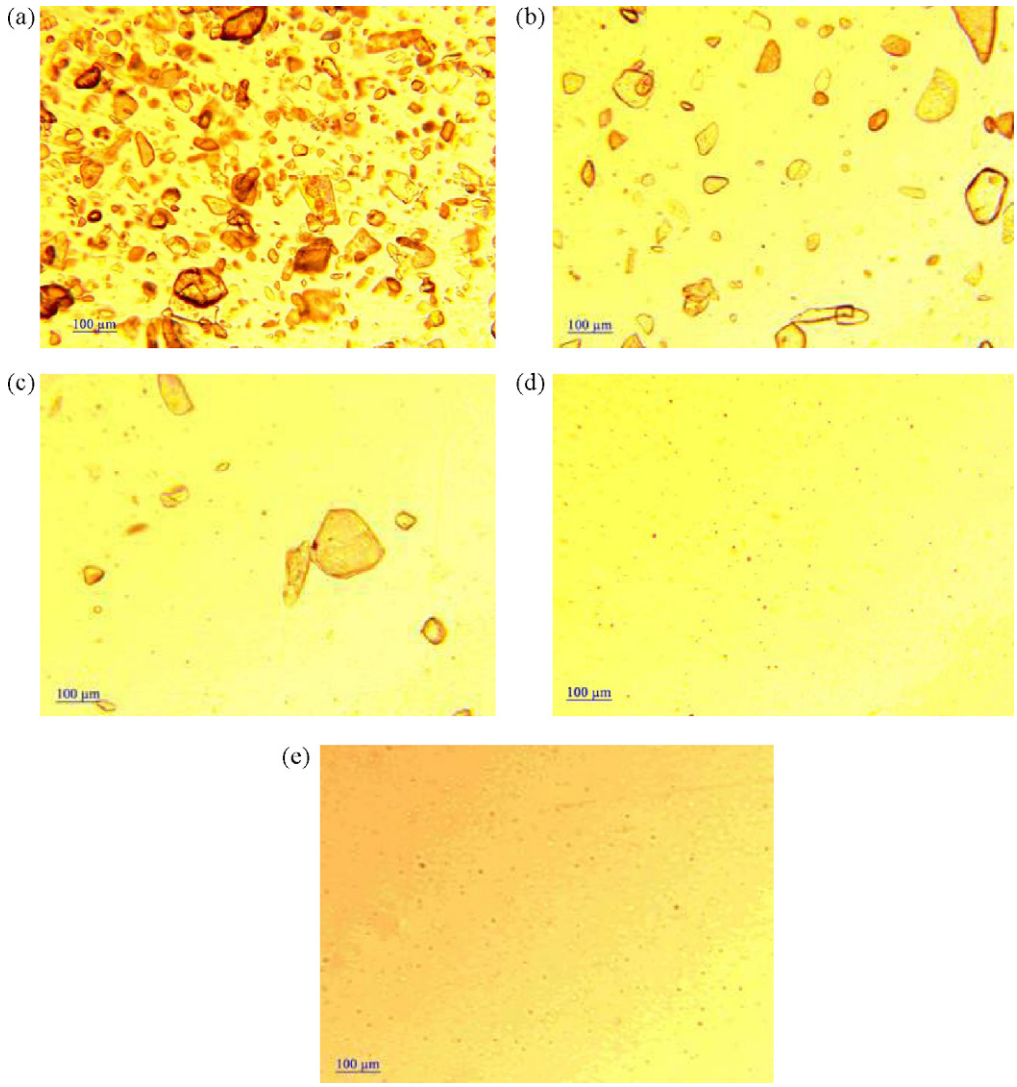

Fig. 7. Optical micrographs of run at 110 °C 100 rpm.

amorphous aggregates, both larger than the critical nucleation size, in the drug–polymer mixture. The drug particulates or amorphous aggregates that were not dissolved into the excipient matrix may act as nucleating agents. By contrast, it may be much more difficult for the drug to precipitate from the supersaturated aqueous solution if the drug–polymer mixture forms a solid solution or if the amorphous aggregates are smaller than the critical nucleation size. This phenomenon can be further explained by nucleation theory. The underlying nucleation mechanism in the former situation is *heterogeneous* nucleation, whereas the mechanism in the latter is *homogeneous* one (Rodriguez-Hornedo and Denette, 1999; Janssens et al., 2008). The energy-barrier for heterogeneous nucleation may be several orders of magnitude lower than that of homogeneous one (Zhai et al., 2006).

In this study, both DSC and XRD showed that the drug were amorphous in the 420 s samples processed at 140 °C 20 rpm, 100 °C 100 rpm and 110 °C 100 rpm. FT-IR analysis not only showed they were amorphous and but also suggested that they could form a solid solution since the asymmetric carboxylic acid C=O stretch peak of cyclic dimmers did not appear. However, the dissolution test showed that there could be some extremely small drug particulates or amorphous aggregates existing in these three samples, and the size of drug particulates or amorphous aggregates in the sample processed at 140 °C 20 rpm was smaller than that processed at 100 °C 100 rpm and 110 °C 100 rpm. The disagreement probably resulted from the sensitivity of FT-IR (Leuner and Dressman, 2000; Qi et al., 2008). It should be emphasized that these small drug particulates or amorphous aggregates which cannot be detected by FT-IR can be nucleating agents and thus result in the physical instability over time during storage.

3.7. Discussion

Specific enthalpy evolution data at different processing conditions are summarized in Fig. 10. All three processing variables used in this study, namely set temperature, counter-rotating twin rotor screw speed, and residence time, are found crucial for the INM's dissolution into the E PO melt. Given the same screw speed of 20 rpm, all INM particles are dissolved into the matrix within 3 min at the highest set temperature of 140 °C employed in this study. At the set temperatures of 100 and 110 °C, the drug particulates are not fully dissolved after 420 s at the lowest rotor screw speed used; increasing the screw speed to 100 rpm allows a full dissolution of drug particulates within 300 s. Obviously, both the setting temperature and screw speed can increase the dissolution rate dramatically.

The dissolution process of the drug in polymer melt is schematically shown in Fig. 11. Firstly, the premixed drug (black) and

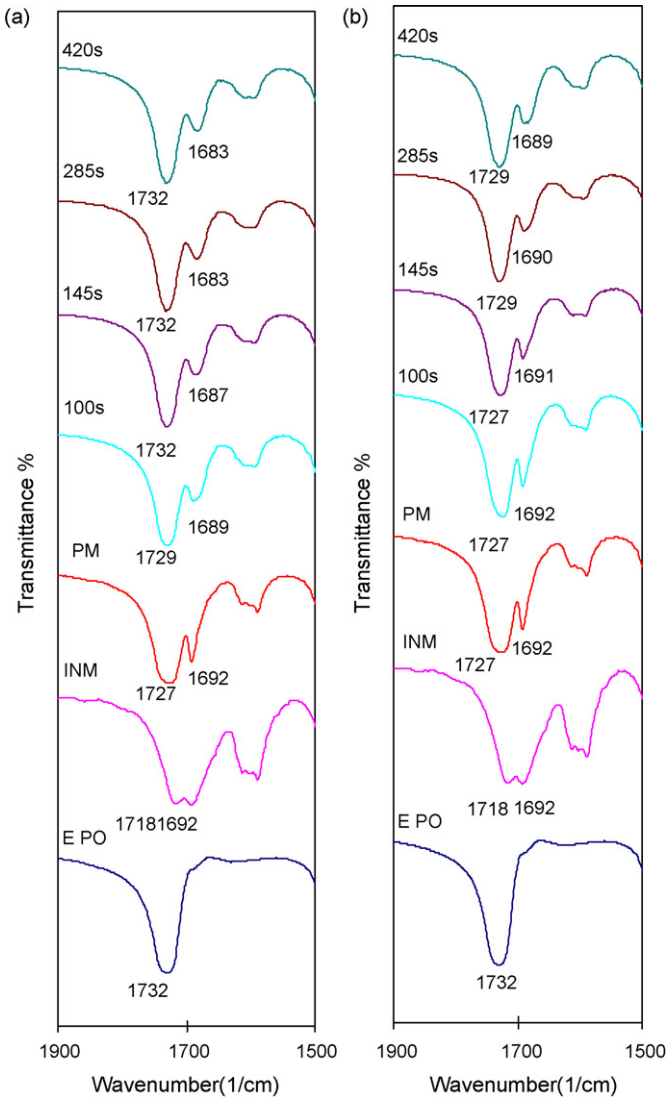

Fig. 8. IR spectra of carbonyl stretching region: (a) 100 °C 100 rpm and (b) 110 °C 20 rpm.

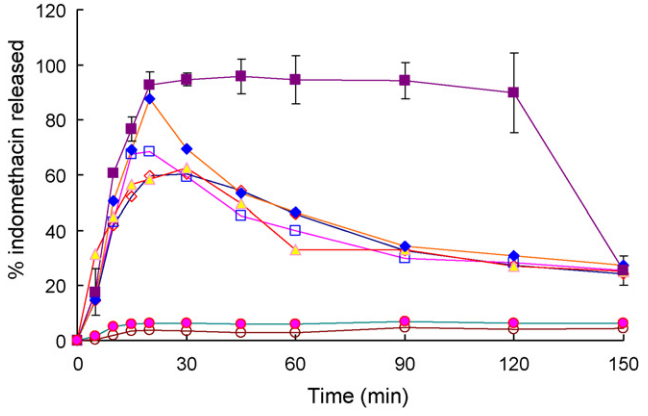

Fig. 9. Dissolution profiles in pH 1.2 buffer solution of runs at: (○) 100% INM; (●) physical mixture; (◊) 100 °C 20 rpm; (△) 110 °C 20 rpm; (□) 100 °C 100 rpm; (♦) 110 °C 100 rpm; (■) 140 °C 20 rpm.

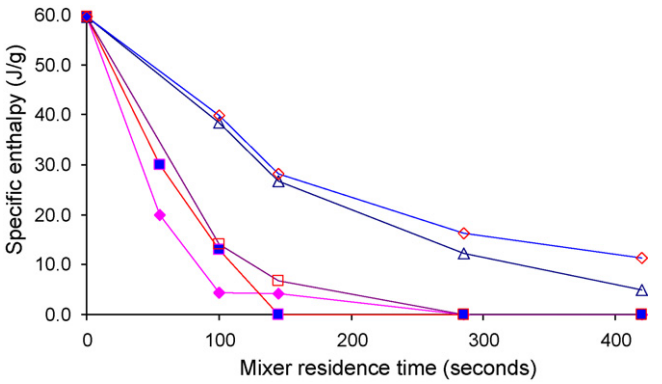

Fig. 10. The evolution of the specific enthalpy with residence time, screw speed and setting temperature: (◊) 100 °C 20 rpm; (△) 110 °C 20 rpm; (□) 100 °C 100 rpm; (♦) 110 °C 100 rpm; (■) 140 °C 20 rpm.

polymer particles (white) are fed into the batch mixer or an extruder. Then, the polymer particles start melting due to the conductive heat from the mixer or extruder barrel and frictional and plastic energy dissipation, leading to the solid drug particles suspended in a continuous polymer melt matrix. After that, the polymer molecules "attack" the drug molecules to create a mass transfer boundary layer around each drug particle, which is continuously wiped away and replaced by fresh polymer melt around each API particulate by the laminar distributive flow of the mixer. The drug molecules diffuse into the polymer melt through the boundary layer, and the size of suspended drug particles diminishes as the diffusion goes on until the particles disappear. Finally, a homogeneous solution is formed.

Thus, the dissolution of the drug in the polymer melt in the batch mixer or an extruder is a forced convective diffusion process, and both dispersive mixing and distributive mixing may significantly enhance the dissolution rate. However, in this study, there was no evidence that dispersive mixing was involved because the size reduction of drug particles was due to the diffusion of the drug molecules to the polymeric melt rather than shear forces. Furthermore, the drug particles do not form agglomerates in the mixture based on the SEM pictures (not shown) of solid mixtures before hot melt processing. Thus, dispersive mixing may *not be needed* in the system studied. Nevertheless, it should be mentioned that, in other drug and polymer systems, dispersive mixing may break up the drug agglomerates or even individual particles due to the high shear forces generated by the high shear screw elements such as wide kneading blocks or Maddock elements (Tadmor and Gogos, 2006). Then, the total surface area of the drug particles exposed to the polymeric melt will be increased, thus increasing the dissolution rate. Miller et al. demonstrated that HME processes can de-agglomerate and disperse "engineered" drug particulates into an excipient matrix without altering their drug properties, and achieving enhanced dissolution properties (Miller et al., 2007). Distributive mixing can homogenize the drug concentration dissolved in the polymeric melt through shear or extensional flow or reorientation, and bring more polymer melt into contact with the suspended drug particles. Both effects keep the driving force, concentration gradient, higher, and thus enhance the dissolution rate. In this study, the effect of distributive mixing was pronounced due to aforementioned reasons. Distributive mixing can be obtained through toothed screw elements or narrow kneading blocks (Manas-Zloczower and Tadmor, 1994; Todd, 1998).

Similarly to the dissolution of drugs in an aqueous medium, the effects of set temperature and screw speed can be further explained by the Noyes–Whitney equation (Noyes and Whitney,

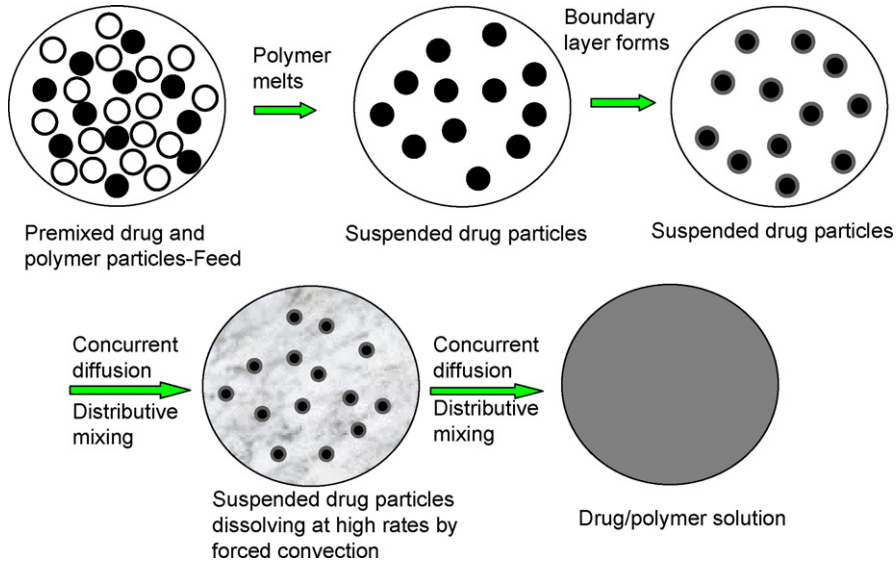

Fig. 11. Schematic representation of the morphological changes of the drug and polymer system in the solution formation process.

1897; Wurster and Taylor, 1965):

$$\frac{dC}{dt} = \frac{D \times A \times (C_S - C)}{h \times V} \quad (1)$$

where D is the diffusion coefficient; A, the total surface area of the drug exposed to the dissolution media; C_S stands for the saturation solubility of the drug in liquid which is polymer melt in the hot melt processing; C describes the concentration of the dissolved solid phase in the bulk at time t; h represents the diffusion boundary layer at the solid–liquid interface; V is the volume of the dissolution medium. If the mixer set temperature increases, on the one hand, the diffusion coefficient will increase due to the increased temperature and resultant decreased matrix viscosity; on the other hand, C_S also will increase. Both of these factors contribute to an increase of the API dissolution rate in the molten polymer excipient. When the screw speed increases, the distributive mixing is improved within the chamber, and thus a higher concentration gradient around the drug particulates is available. Moreover, the thickness of mass transfer boundary layer decreases as the screw speed increases. Both effects lead to an increased dissolution rate.

The experimental results also lead to an important finding which has been overlooked before: the times needed for the drug to dissolve inside the polymer melt and the typical residence time for an extrusion process can be *comparable*, under appropriate processing conditions. Depending on the set temperature and the screw speed, the drug dissolution process may take one to a few minutes. The residence time of a typical continuous manufacturing extrusion process falls in the same range (Gao et al., 2000; Cassagnau et al., 2005). Hence, the batch internal mixer results obtained in this work are relevant to the expected performance of the API/excipient system in hot melt extrusion (HME) processes currently being used, or under evaluation by the pharmaceutical industry. Furthermore, the HME process offers the possibility of further shortening the residence time to fully dissolve INM particulates into the molten E PO, through the liberal use of screw distributive or dispersive elements. On the other hand, one has to be careful when optimizing the HME process parameters such as screw speed, feeding rate and barrel temperature, because changes in those parameters may lead to a change of the processing stream's residence time. Finally, split feeding, i.e., feeding the drug particles from a port downstream to minimize adverse thermal effects on the API, may not be a good choice in some cases due to the sacrifice in the residence time.

4. Conclusions

The dissolution of INM solid particles into molten E PO was studied through processing the mixture in a batch laminar mixer at various temperatures below the melting point of the API. Set temperature, rotor screw speed, and residence time were found to be critical for the dissolution of the drug into the molten polymer matrix. The dissolution of drugs in polymeric melt is a convective diffusion process, and the dissolution rate can be enhanced by increasing set temperature and screw speed. The time needed for the drug to dissolve into the molten polymer in the batch mixer and the typical residence time for common single and twin extrusion processes appear to be comparable. Hence, the results of this study are directly applicable to the HME pharmaceutical processes run at the temperatures employed.

Acknowledgements

Four of the authors received support from the ongoing US Department of the Army, DAAE30-03-D1015 *Advanced Cluster Energetics* (ACE^{TM}) Program at New Jersey Institute of Technology (NJIT). This research was financially supported by National Science Foundation under Grant CMMI-0927142. The authors want thank their colleagues at the NJIT/PPI HME Processing, Scale-up, and Product Characterization Laboratory, Prof. Marino Xanthos and Dr. Kuanyin Lin, Dr. Linjie Zhu and JinUk Ha for their significant input and insightful discussions related to this article.

References

Breitenbach, J., 2002. Melt extrusion: from process to drug delivery technology. Eur. J. Pharm. Biopharm. 54, 107–117.
Cassagnau, P., Courmont, M., Melis, F., Puaux, J.P., 2005. Study of mixing of liquid/polymer in twin screw extruder by residence time distribution. Polym. Eng. Sci. 45, 926–934.
Chokshi, R.J., Sandhu, H.K., Iyer, R.M., Shah, N.H., Malick, A.W., Zia, H., 2005. Characterization of physico-mechanical properties of indomethacin and polymers to assess their suitability for hot-melt extrusion process as a means to manufacture solid dispersion/solution. J. Pharm. Sci. 94, 2463–2474.
Chokshi, R.J., Shah, N.H., Sandhu, H.K., Malick, A.W., Zia, H., 2008. Stabilization of low transition temperature indomethacin formulations: impact of polymer-type and its concentration. J. Pharm. Sci. 97, 2286–2298.
Crowley, M.M., Zhang, F., Repka, M.A., Thumma, S., Upadhye, S.B., Battu, S.K., McGinity, J.W., Martin, C., 2007. Pharmaceutical applications of hot-melt extrusion. Part I. Drug Dev. Ind. Pharm. 33, 909–926.
Filippis, P.D., Boscolo, M., Gibellini, M., Rupena, P., Rubessa, F., Moneghini, M., 1991. The release rate of indomethacin from solid dispersions with Eudragit E. Drug Dev. Ind. Pharm. 17, 2017–2028.

Fujii, M., Okada, H., Shibata, Y., Teramachi, H., Kondoh, M., Watanabe, Y., 2005. Preparation, characterization, and tableting of a solid dispersion of indomethacin with crospovidone. Int. J. Pharm. 293, 145–153.
Gao, J., Walsh, G.C., Bigio, D., Briber, R.M., Wetzel, M.D., 2000. Mean residence time analysis for twin screw extruders. Polym. Eng. Sci. 40, 227–237.
Ghebre-Sellassie, I., Martin, C., 2007. Pharmaceutical Extrusion Technology. Informa Healthcare, New York.
Hulsmann, S., Backenfeld, T., Keitel, S., Bodmeier, R., 2000. Melt extrusion-an alternative method for enhancing the dissolution rate of 17β-estradiol hemihydrate. Eur. J. Pharm. Biopharm. 49, 237–242.
Janssens, S., Nagels, S., Armas, H.N.D., Autry, W.D., Schepdael, A.V., Mooter, G.V.D., 2008. Formulation and characterization of ternary solid dispersions made up of Itraconazole and two excipients, TPGS 1000 and PVPVA 64, that were selected based on a supersaturation screening study. Eur. J. Pharm. Biopharm. 69, 158–166.
Kistenmacher, T.J., Marsh, R.E., 1972. Crystal and molecular structrure of an anti-inflammatory agent, indomethacin 1-(p-chlorobenzoyl)-5-methoxy-2-methylindole-3-acetic acid. J. Am. Chem. Soc. 94, 1340–1345.
Leuner, C., Dressman, J., 2000. Improving drug solubility for oral delivery using solid dispersions. Eur. J. Pharm. Biopharm. 50, 47–60.
Lin, S.Y., Perng, R.I., 1993. Solid-state interaction studies of drugs/polymers. I. Indomethacin/Eudragit E, RL or S resins. S.T.P. Pharma. Sci. 3, 465–471.
Manas-Zloczower, I., Tadmor, Z., 1994. Mixing and Compounding of Polymers. Hanser Publishers, Munich.
Marsac, P.J., Li, T.L., Taylor, L.S., 2009. Estimation of drug–polymer miscibility and solubility in amorphous solid dispersions using experimentally determined interaction parameters. Pharm. Res. 26, 139–151.
Miller, D.A., McConville, J., Yang, W., Williams III, R.O., McGinity, J.W., 2007. Hot-melt extrusion for enhanced delivery of drug particles. J. Pharm. Sci. 96, 361–376.
Nakamichi, K., Nakano, T., Yasuura, H., Izumi, S., Kawashima, Y., 2002. The role of the kneading paddle and the effect of screw revolution speed and water content on the preparation of solid dispersions using a twin-screw extruder. Int. J. Pharm. 241, 203–211.
Noyes, A.A., Whitney, W.R., 1897. The rate of solution of solid substances in their own solutions. J. Am. Chem. Soc. 19, 930–934.
Qi, S., Gryczke, A., Belton, P., Craig, D.Q.M., 2008. Characterization of solid dispersions of paracetamol and EUDRAGIT E prepared by hot-melt extrusion using thermal, microthermal and spectroscopic analysis. Int. J. Pharm. 354, 158–167.
Repka, M.A., Battu, S.K., Upadhye, S., Thumma, S., Crowley, M.M., Zhang, F., Martin, C., McGinity, J.W., 2007. Pharmaceutical applications of hot-melt extrusion. Part II. Drug Dev. Ind. Pharm. 33, 1043–1057.
Rodriguez-Hornedo, N., Denette, M., 1999. Significance of controlling crystallization mechanisms and kinetics in pharmaceutical systems. J. Pharm. Sci. 88, 651–660.
Shibata, Y., Fujii, M., Sugamura, Y., Yoshikawa, R., Fujimoto, S., Nakanishi, S., Motosugi, Y., Koizumi, N., Yamada, M., Ouchi, K., Watanabe, Y., 2009. The preparation of a solid dispersion powder of indomethacin with cropovidone using a twin-extruder or kneader. Int. J. Pharm. 265, 53–60.
Slavin, P.A., Sheen, D.B., Shepherd, E.E.A., Sherwood, J.N., Feeder, N., Docherty, R., Milojevic, S., 2002. Morphological evaluation of the γ-form of indomethacin. J. Cryst. Growth 237–239, 300–305.
Tao, J., Sun, Y., Zhang, G.G.Z., Yu, L., 2009. Solubility of small-molecule crystals in polymers: D-mannitol in PVP, indomethacin in PVP/VA, and nifedipine in PVP/VA. Pharm. Res. 26, 855–864.
Tadmor, Z., Gogos, C.G., 2006. Principles of Polymer Processing, 2nd ed. Wiley-Interscience, New Jersey.
Taylor, L.S., Zografi, G., 1997. Spectroscopic characterization of interactions between PVP and indomethacin in amorphous molecular dispersions. Pharm. Res. 14, 1691–1698.
Todd, D.B., 1998. Plastics Compounding Equipment and Processing. Hanser Publisher, New York.
Verreck, G., Decorte, A., Heymans, K., Adriaensen, J., Liu, D., Tomasko, D., Arien, A., Peeters, J., Van den Mooter, G., Brewster, M.E., 2006. Hot stage extrusion of p-amino salicylic acid with EC using CO_2 as a temporary plasticizer. Int. J. Pharm. 327, 45–50.
Wurster, D.E., Taylor, P.W., 1965. Dissolution rates. J. Pharm. Sci. 54, 169–175.
Zhai, W.T., Yu, J., Wu, L.C., Ma, W.M., He, J.S., 2006. Heterogeneous nucleation uniformizing cell size distribution in microcellular nanocomposites foams. Polymer 47, 7580–7589.
Zhu, Y., Shah, N.H., Malick, A.W., Infeld, M.H., McGinity, J.W., 2006. Controlled release of a poorly water-soluble drug from hot-melt extrudates containing acrylic polymers. Drug Dev. Ind. Pharm. 32, 569–583.